THE ROLE OF EMBEDDED CLUSTERS IN STAR FORMATION

ELIZABETH A. LADA
Department of Astronomy
University of Florida
211 Bryant Space Science Building
Gainesville, FL 32608 USA

1. Introduction

During the past century, astronomers have discovered that star formation is a continuous, ongoing process, occurring over the lifetime of our Galaxy and the universe. However, how stars form, still remains a mystery. Unraveling the process of stellar birth is of fundamental importance for understanding not only the origin of stars but also the origin and evolution of planets, life and even galaxies. For example, since stars are the basic constituents of galaxies, stellar formation and evolution are the engines that drive galaxy evolution. Once stars form, astronomers can use the elegant theory of stellar structure and evolution to predict the life histories of galaxies. However a comparable theory of star formation does not currently exist and therefore limits any future progress toward understanding galaxy evolution.

The reason that the process of stellar birth has remained a mystery for much of this century has to do with where stars form. Stars form deep within molecular clouds. The prenatal gas in these clouds is very cold and therefore emits only at millimeter and radio wavelengths. The clouds also contain large amounts of dust which surround forming stars, rendering them invisible at optical wavelengths. Consequently, the star forming process can not be observed via traditional methods of optical astronomy. Luckily, advances in observational technology over the last two decades, especially at millimeter and infrared wavelengths have permitted the direct observation of star forming regions. As a result many new and surprising discoveries about the star forming process have been uncovered. One such discovery is that rich embedded clusters, containing hundreds of newly formed stars, are more numerous than previously suspected. In fact, they may account for most of the star formation, independent of mass, occurring in our Galaxy.

As we will discuss, the dense environments forming embedded clusters are quite different from regions forming only one or two isolated stars. Therefore one might expect to find fundamental differences in the physics of not only the star forming process but also the early evolution of young stars and their planets. In the following sections, I will discuss the role that young embedded cluster have in our attempts to understand the origins of stars and planets.

2. The Distribution of Star Formation in Giant Molecular Clouds

"The current views of stellar evolution allow us to date galactic clusters on the basis of their color-magnitude diagrams. The youngest known clusters, those containing O-type stars, are at most a few million years old. Obviously such clusters must be continually forming unless we are at the unlikely epoch when star formation has ceased. It would be important to know if these clusters and associations represent the only regions of star formation or whether individual stars may form in the general field. " - Roberts 1957

Over the past decade, observations of nearby star forming regions have led to the suggestion that two distinct modes of star formation may exist, (1) a distributed, loosely aggregated or isolated mode and (2) a clustered, tightly packed or grouped mode. Distributed or isolated star formation can be characterized by low stellar density and low overall star formation efficiency. In this mode, one to a few stars form in single, low mass, dense cores distributed throughout a molecular cloud. An example of this mode is seen in the Taurus molecular cloud, where $\sim$ 100 stars are forming over a 300 pc^2 area from $\sim 10^4$ M$_\odot$ of gas. In contrast, the clustered mode of star formation is characterized by high stellar densities and relatively high star formation efficiency. In this mode, groups of stars form from a massive concentration of gas. An example of clustered star formation is seen in the Rho Ophiuchus cloud core where 100 stars form over a 2 pc^2 region from $\sim$ 600 M$_\odot$ of gas.

To determine the relative contributions of each of these modes of star formation to the current star forming activity in our Galaxy and thereby answer the question posed by Roberts, requires a thorough and systematic census of the youngest stellar populations in giant molecular clouds. Such surveys are best done at infrared wavelengths. Remember, molecular clouds are full of dust. This dust absorbs and scatters radiation from x-rays to infrared wavelengths (Mathis 1990) and hence renders the clouds and their new born stars nearly invisible at optical wavelengths. Luckily, the nature of the dust (e.g. size and type of grain) which is responsible for the observed extinction of light through the clouds, is such that it produces a continuous decrease in this extinction with increasing wavelength. Figure 1 shows the

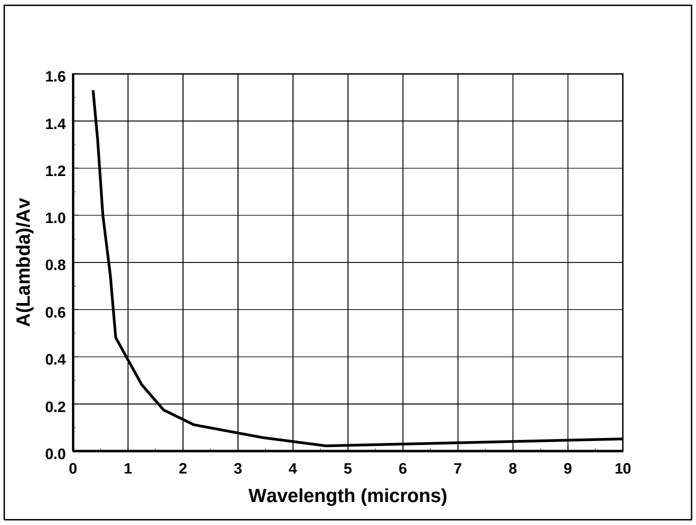

Figure 1. The infrared extinction law. This figure was constructed using the data from the paper of Rieke & Lebofsky (1985).

extinction law measured by Rieke and Lebofsky (1985) for wavelengths ranging from 0.2 to 10 microns. From this figure, one can see a marked decrease in extinction from optical to infrared wavelengths. For example, the extinction at 2.2 μm is roughly a factor of 10 less than the extinction measured at visual wavelengths.

Advances in infrared detector technology have enabled us to probe the dusty interiors of molecular clouds and directly study their stellar progeny. For example, the IRAS satellite provided a flux-limited census of far-infrared sources in giant molecular clouds (GMCs). This data base was used for some of the first comprehensive studies of the distribution of young stellar objects in nearby molecular clouds such as Taurus (Kenyon et al. 1990). However, since the IRAS survey had limited sensitivity and young stars are typically weak far-infrared emitters, the majority of young stellar objects in all but the nearest molecular clouds ($\sim$ 100 pc), could not be detected by IRAS. In addition, the angular resolution of IRAS is coarse and consequently many star forming regions suffer from confusion due to source crowding. The recent development of sensitive, large format imaging arrays at near-infrared wavelengths has alleviated such problems and made it possible, for the first time, to search large areas of molecular clouds for their embedded stellar populations at unprecedented sensitivi-

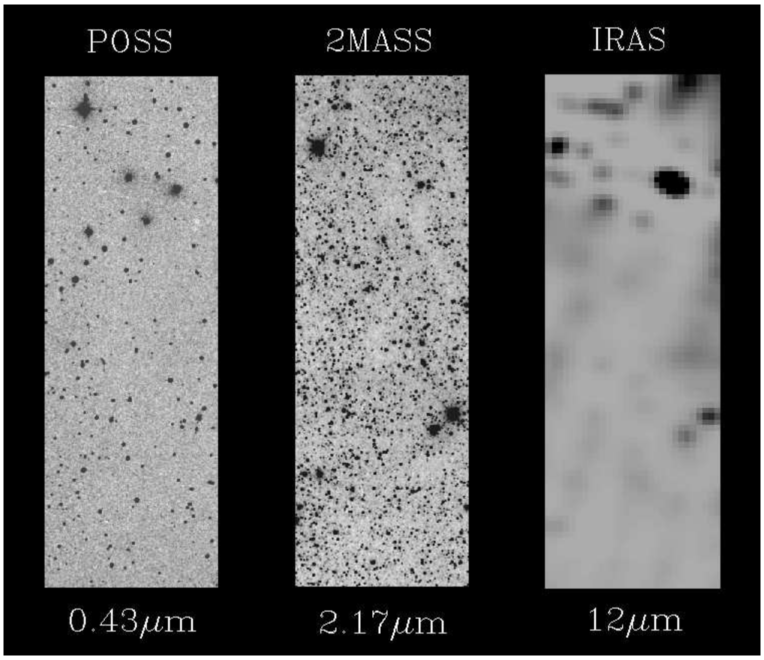

Figure 2. Comparison of an image of the sky taken at optical (POSS), near-infrared (2MASS) and mid-infrared (IRAS) wavelengths. This figure illustrates the advantage of near-infrared imaging observations for obtaining a thorough census of young objects.

ties and resolutions. Figure 2 compares an optical POSS image with a 2 micron image of the same field from the 2MASS survey and a 12 micron image from IRAS. The near-infrared observations clearly detect many more sources than either the optical or IRAS observations.

While, near-infrared imaging observations are the most effective means of obtaining a census of the youngest stellar populations in molecular clouds, they do have their own limitations. Namely, near-infrared surveys can be contaminated by field stars, in front of and behind the molecular clouds and can also suffer from background source confusion at very faint magnitudes. The general field star population consists mainly of late type dwarf and giants (Figure 3). These late type dwarfs and giants are bright at near-infrared wavelengths (Figure 4). Given the reduced extinction at these wavelengths such stars can contribute significantly to star counts obtained at 2 microns, even when they are observed through an intervening molecular cloud. It is therefore essential to account for the distribution of background field stars before assessing the young stellar content of the clouds. The most common and straight-forward way to determine the conch

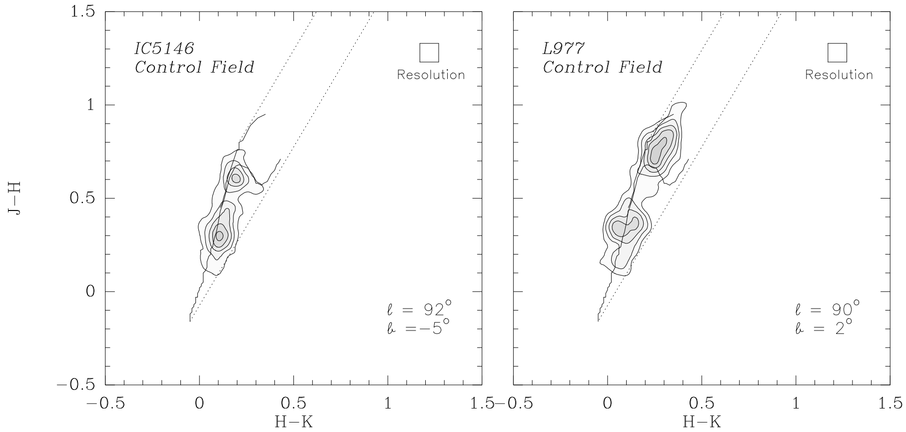

Figure 3. Near-infrared (JHK) color-color diagrams for control (off) fields for the IC 5146 and L977 molecular clouds. The contours represent the surface density of stars in the JHK color-color plane. The dwarf and giant sequence (solid line) and the reddening vector (dashed line) are shown. This figure is from Alves et al., (1998)

tribution of field stars to a near-IR survey is to obtain star counts of control fields, large areas located nearby but off the cloud. By appropriately scaling the area of these control fields to match the area surveyed on the cloud, one can determine the membership of young stars in the cloud on a statistical basis. However, determining whether or not a specific star in the region is associated with the molecular cloud or is a field star is not possible by this method. In order to determine the membership of individual sources requires additional information, such as stellar proper motions, spectra, multi-color near-IR photometry or 2.3 μm CO narrow band photometry.

The first cloud to be systematically surveyed at near-infrared wavelengths was the L1630 molecular cloud (Lada et al. 1991). Approximately 0.8 square degrees of the cloud was observed at 2.2 μm to a completeness limit of 13^{th} magnitude (Figure 5). The region surveyed was contained within the molecular cloud boundaries and roughly half of the area surveyed contained CS emission from dense gas and the remaining half did not. The survey was sensitive enough to sample both high and low mass stars and in particular to detect stars with masses comparable or less than the sun. The survey identified four embedded clusters, NGC 2024, NGC 2071, NGC 2068 and NGC 2023 within the cloud. These clusters are associated with previously known regions of star formation. The spatial distribution of the stars in L1630, shown in Figure 5, is highly concentrated. More than half the near-infrared sources detected were contained in the three most populous embedded clusters, NGC 2071, NGC 2068, NGC 2024. The sizes of these 3 clusters cover less than 18% of the cloud area surveyed, indicating that

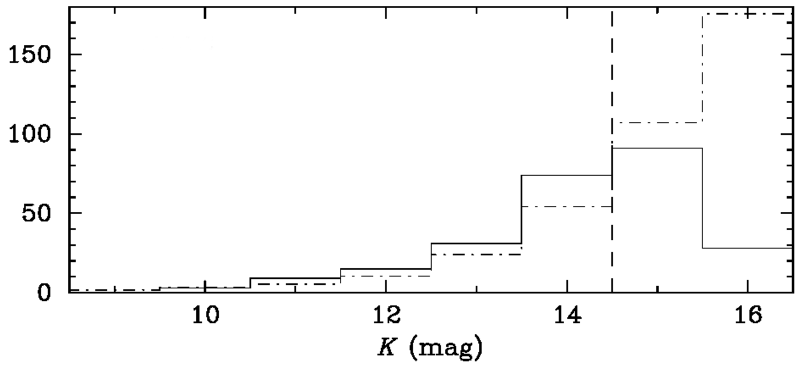

Figure 4. The observed K magnitude distribution of background sources for control fields near the L1630 molecular is shown as a histogram (solid line). Also shown are model estimates of the the field star distribution. This figure was taken from Li et al. (1999).

star formation occurs in very localized regions. In addition, the number of stars found outside the clusters is consistent with the expected number of background stars not associated with the cloud. After correcting for the presence of field stars, it was estimated that the vast majority ($\sim$ 96%) of the stars in the L1630 molecular cloud were formed within these three rich clusters!

Could there be a significant distributed population in L1630? Recently, Li, Evans & Lada (1997, 1999) addressed this question by searching for a distributed population of pre-main sequence stars in the cloud. They surveyed a 1320 arcmin^2 region of L1630, at J, H, and K. The region surveyed concentrated on an area that was away from the dense molecular cores and that exhibited modest visual extinctions ($\leq$ 10 mag) (Figure 6). Two different approaches, a near-infrared color analysis and a star counting analysis, were used to look for a distributed population. Since young stars are surrounded by large amounts of gas and dust, they radiate a significant fraction of their energy at infrared wavelengths and consequently many young PMS stars have near-infrared emission in excess of their photospheric emission. Therefore one can search for evidence of recent star formation by looking for sources exhibiting near-infrared excess. Using this method, Li, Evans & Lada (1997) estimated that the fraction of sources, located outside the cluster, with near-infrared excess is 3% - 8%. In addition, the surface density of near-infrared excess sources is 1/7 of that found in the distributed population of L1641 and 1/20 of that found in the low density, young clus-

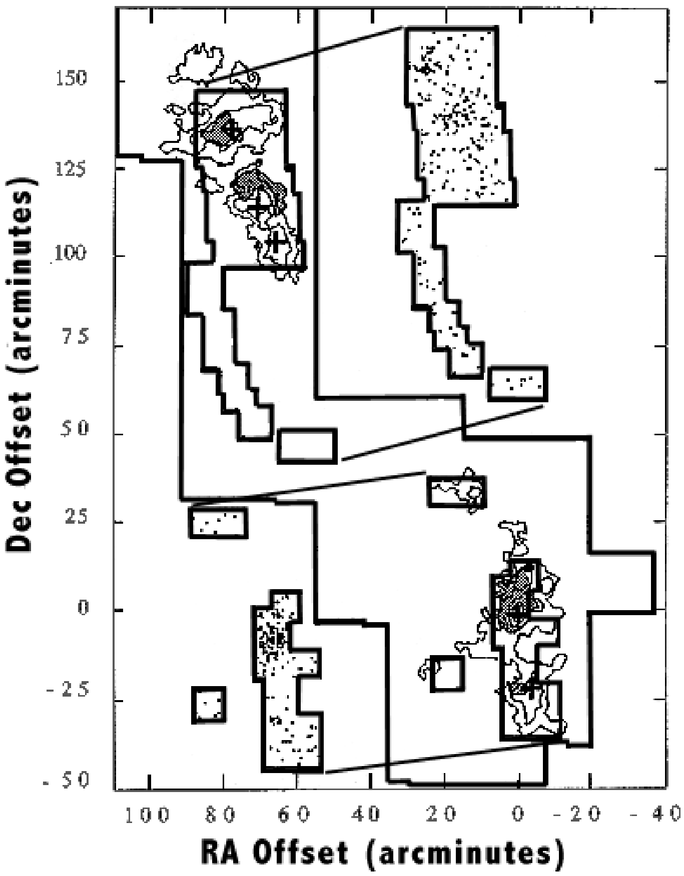

Figure 5. K-band survey of L1630 adapted from Lada et al. (1991) and Lada (1992). The survey boundaries are overlaid on a contour map of the CS(J=2-1) survey (outer boundary). The shaded areas indicate the cluster boundaries. The distribution of K-band sources with $m_K < 13$ is also shown in the in-set boxes. The (0,0) position corresponds to $\alpha = 5^h\ 39^m\ 12^s$ and δ = -01^o 55$'$ 42$''$.

ter NGC 2023. The low fraction and low surface density of excess sources indicates that recent star formation activity has been very low in the outlying regions of L1630. The second approach used to search for a distributed population, employed near-infrared star counts (Li, Evans & Lada 1999). Extensive and carefully studied control fields, off the molecular cloud, were used to establish the stellar surface densities of field stars and a method was developed using the survey data and a ^{13}CO map to extract field stars not associated with the cloud. Comparison of the star counts of the control fields with the on-cloud fields reveals no evidence for a distributed population (Figure 6). Results from both the near-infrared color analysis and star counting analysis both confirm and strongly support the earlier conclusions that *most stars in L1630, independent of mass, formed in a clustered mode of star formation, similar to the star formation process in the Rho Ophiuchi cloud core* (Lada 1992).

If L1630 is a typical GMC, then most stars in the Galaxy may have formed in embedded clusters, not in isolation. Indeed near infrared imaging observations of GMCs have revealed the existence of a large number of young embedded clusters (e.g. Lada et al. 1993; Zinnecker et al. 1993). However, only a few molecular clouds have been systematically surveyed to the appropriate sensitivities to empirically test whether or not most stars form in cluster environments. One cloud that has been extensively studied for its young stellar content is the L1641 molecular cloud. L1641 is also part of the Orion complex and is only located several degrees south of L1630. Strom, Strom & Merrill (1993) found a population of isolated pre-main-sequence (PMS) stars distributed throughout the cloud. The origin of this distributed population is unclear at this time. Based on spectroscopic studies, Allen (1996) suggested that as much as half of the stars in L1641 (excluding OMC1-2) may have formed in relative isolation, distributed through the cloud. This population may therefore have formed in a similar manner to stars in the Taurus dark cloud. Is a distributed mode of star formation more prevalent in L1641? In addition to the distributed population of young stars, a number of rich clusters also have been identified in L1641 and several examples of these clusters are shown in Figure 7. These include the famous Trapezium cluster, and a number of embedded clusters found in the near-IR survey of Strom, Strom and Merrill (1993). The clusters found in L1641 have properties very similar to the clusters in L1630 (see Section 3, Table 1). Therefore the clustered mode of star formation also appears to be significant in this cloud. Meyer and Lada (1999) recently examined the published studies of the young stellar population in L1641 to assess the relative contributions of the clustered and distributed modes of star formation and to compare the star forming activity in L1641 with that in L1630. When they considered the entire stellar population, including the OMC region, they estimated that $> 2/3$ of the total number of stars < 10 Myr old are part of rich clusters (also see Lada, Strom & Myers 1993). They concluded that the star forming activity in L1641 is similar to that in L1630 and that in both clouds, *most stars form as part of young clusters compared to a minority that form in relative isolation.*

In addition to the studies in Orion, the cluster mode of star formation

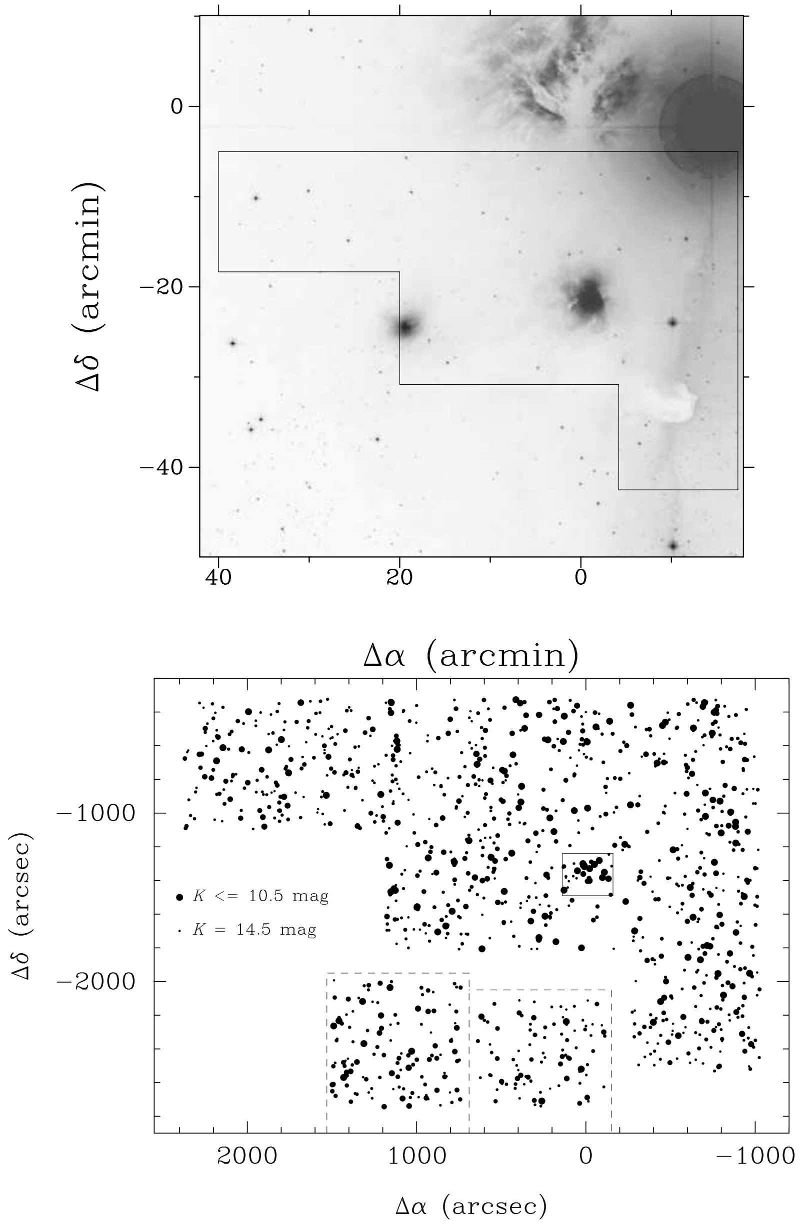

Figure 6. Region of the L1630 molecular cloud surveyed at J, H and K by Li, Evans & Lada (1997, 1999) (Top Panel). The distribution of stars with K< 14.5 is shown in the bottom panel. For comparison, the distribution of field stars from control fields off the cloud are shown in the 2 dotted-lined inserts

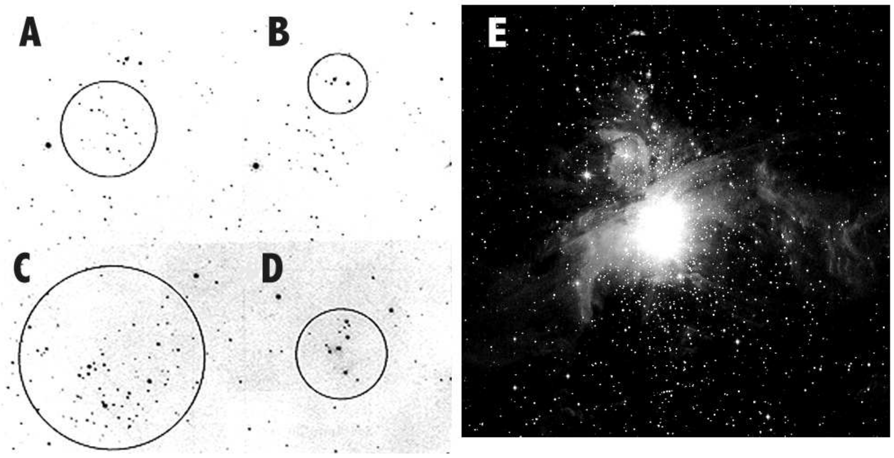

Figure 7. Clusters in the L1641 molecular clouds. On the left, 4 young clusters, L1641 C (A), KMS 36 (B) L1641 S (C) and CK Group (D) are shown. These clusters were identified from the near-infrared survey by Strom, Strom & Merrill (1993). On the right, a JHK composite image of the Trapezium cluster in L1641, courtesy of the 2MASS Survey is presented.

appears to contribute significantly to the star forming process in other molecular clouds. A recent J, H, K survey of roughly a square degree of the Rosette molecular cloud revealed the existence of at least seven embedded clusters in the RMC, five of which were previously unknown (Phelps & Lada, 1997). The locations of these clusters within the molecular cloud is shown in Figure 8. Sensitive follow-up observations of several of the Rosette clusters have shown them to be similar in richness to the L1630 clusters (Lada, Muench, Phelps, 1999 in prep.) Embedded cluster formation has also been found to be significant in the Gemini OB 1 cloud (Carpenter, Snell & Schloerb, 1995), NGC 2264 (Lada, et al. 1990), IC 5146 (Lada, et al. 1993). However, while clusters have been shown to be numerous in these other molecular clouds, most current observations are not sensitive or extensive enough to determine whether cluster formation is responsible for producing most of the stars in the clouds. Finally, even in regions, where the distributed mode of star formation was thought to dominate, such as the Taurus molecular clouds, clustering is also found to be important. Gomez et al. 1993 investigated the distribution of pre-main sequence stars in Taurus via the two-point correlation function and the nearest-neighbor analysis and found that young stars in Taurus preferentially form in small groups. As we shall see in Section 3, the basic properties of these small Taurus clusterings differ from the properties of the embedded clusters typically found in GMCs.

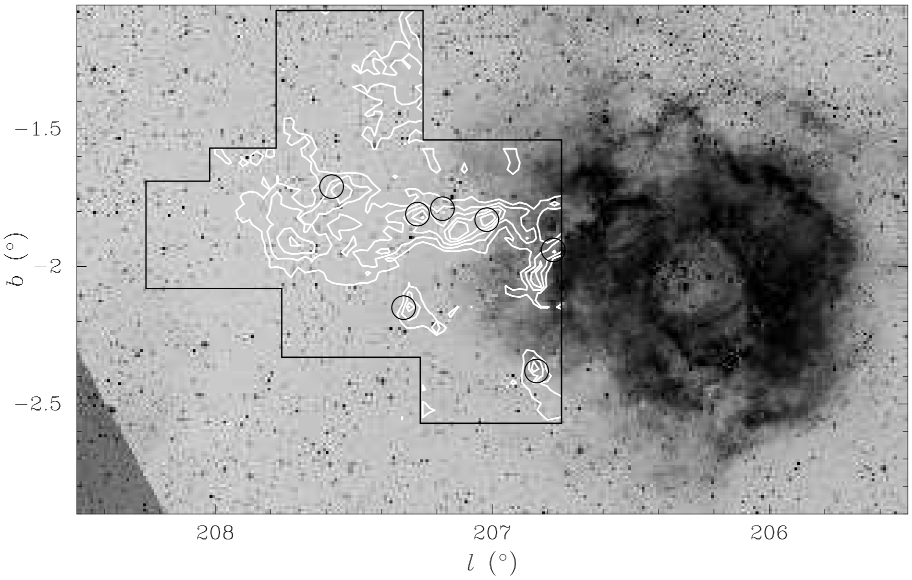

Figure 8. The distribution of ^{13}CO gas (white contours) (Blitz & Stark 1986) and the location of embedded clusters (open circles) (Phelps & Lada 1997) in the Rosette Molecular cloud is overlaid on the Digital Sky Survey image of the Rosette region. The Digitized Sky Survey was produced at the Space Telescope Science Institute.

3. Properties of Embedded Clusters

3.1. DEFINITION & IDENTIFICATION OF EMBEDDED CLUSTERS

Before reviewing the properties of embedded clusters, it is useful to first define what an embedded cluster is. Empirically, a cluster or an association is defined as: *a group of stars of the same physical type whose surface density significantly exceeds that of the field for stars of the same physical type.* Clusters are distinguished from associations by their higher stellar space densities. To distinguish clusters from multiple star systems we arbitrarily require that a cluster consist of more than 10 members. Clusters can be characterized by their richness: clusters with 100 or more members are designated as rich and those with less than 100 members as poor. Further clusters as defined above can be classified into two environmental classes depending on their association with interstellar material. *Embedded clusters* (the subject of this review) are clusters which are fully or partially embedded in the interstellar gas and dust. Exposed clusters are clusters with little or no interstellar material within their boundaries. This basic definition of a cluster includes stellar systems of two dynamical states: bound and unbound. Bound clusters are systems whose total energy (kinetic + potential) is negative. Unbound clusters have total energies which are positive. Note, when determining the total energy, we include contributions from any interstellar material contained within the boundaries of the clusters. For a more in depth definition of clusters the reader is referred to the review by Lada & Lada (1991).

Infrared observations of molecular clouds are needed to reveal the presence of embedded clusters since many, if not all members will be heavily obscured. The initial identification of an embedded cluster is typically made by a survey at a single infrared wavelength or color, typically 2.2 μm or K-band. The existence of an embedded cluster is established by an excess density of stars of a given type (e.g. bright 2.2 μm sources) over the background. For example, the insets in Figure 5 show the location of the K-Band (K$<$ 13) infrared sources detected in a survey of the L1630 GMC. About 1000 sources are present. Their distribution on the sky is not uniform and over half the sources are located in four well defined clusters as discussed in the previous section. These clusters are also shown in Figure 5 as shaded contours or regions overlaid on the CS(J=2-1) map. The boundaries of the shaded cluster regions correspond to a source surface density which is ten times that of the background. Here, star counts clearly reveal the presence of embedded clusters. In general, the ease of identifying an embedded cluster depends sensitively on the richness of the cluster, the apparent brightness of its members, its angular size or compactness, its location in the galactic plane, and the amount of obscuration in its direction. For example, it would be difficult to recognize a spatially extended, poor cluster of faint stars located in a direction where there is a high background of infrared sources.

3.2. STELLAR DENSITIES AND STRUCTURE

Once a cluster is identified, some basic properties can be determined. Table 1 summarizes the properties of several nearby embedded clusters. Embedded clusters exhibit high stellar surface densities. Typically these young clusters will have a few hundred to a few thousand stars per square parsec within their boundaries. Such densities are much higher than the surface densities for classical open clusters like the Pleiades or more distributed regions of star formation like Taurus (Gomez et al. 1993).

In general, the distribution of stars within a cluster is centrally condensed. The variation in surface density in young clusters such as the Trapezium (McCaughrean & Stauffer 1994), IC 348 (Lada & Lada 1995) and NGC 2282 (Horner, Lada & Lada 1997) falls off roughly as r^{-1}. Figure 9 shows the radial density profile of the K band sources for the NGC 2282 cluster. The best fit to the data is a r^{-1} power-law, represented in Figure

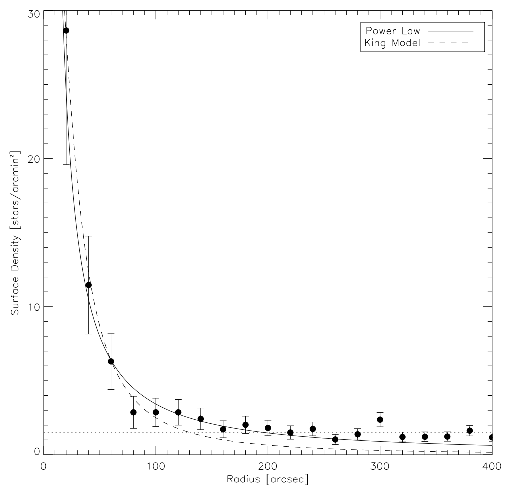

Figure 9. Radial surface density profile of the NGC 2282 cluster. The dotted horizontal line corresponds to the density of field stars in this region. The power-law fit (solid line) gives a r^{-1} dependence while the King model (dashed line) gives a core radius of 0.19 pc. (From Horner, Lada & Lada, 1997)

9 as a solid line. For comparison a King model of the form $f(r) = f_0[1 + (r/r_c)^2]^{-1}$ is shown. It also fits the data fairly well. In addition to being centrally condensed, young embedded clusters also show evidence of significant structure and sub-clustering. Figure 10 presents the K-band image and corresponding contour map of the stellar surface density distribution for the IC 348 cluster located in the Perseus molecular cloud (Lada & Lada 1995). The lowest contour level in this figure corresponds to the estimated surface density of field stars in this region and subsequent levels are multiples of this value. The lowest solid contour level represents a surface density of three times the estimated field star density. Most of the stars in IC 348 are found in a large central concentration. However, outside this main cluster, eight smaller, but significant sub-clusterings can be readily identified. The stellar surface densities of these smaller sub-clusters are high, ranging from 70 - 270 stars pc^{-2}, typical of the overall densities of embedded clusters and more than an order of magnitude larger than the small clusters in the Taurus cloud (Gomez et al. 1993). In addition, the densities of the sub-clusters are consistent with those expected from a r^{-1} falloff in the overall surface density of the cluster and may be a result of expected statistical fluctuations in the outwardly decreasing surface density distribution of the cluster.

Table 1: Embedded Cluster Properties

Cluster	Average Properties			Central 0.1 pc Radius	
	Number of Stars	Radius (pc)	Stellar Density pc^{-2}	Number of Stars	Stellar Density pc^{-2}
NGC 2023	21	0.3	100		
NGC 2071	105	0.6	132		
NGC 2068	192	0.9	112		
NGC 2024	300	0.9	172	50	1600
L1641 S	134	1.3	100		
CK Group	25	0.7	72		
Trapezium	700	0.5	1000	98	3100
	1600	2.5	89		
IC 348	345	1.0	105	30	955
NGC 1333	275	0.5	140		
Taurus	9−15	0.5−1.1	5−14	1−few	30-90

It is interesting to consider the stellar densities of embedded clusters on the 0.1 pc scale of their central regions. A 0.1 pc radii corresponds to the size scale expected for the protostellar envelope of a single star (Adams et al. 1987) and also the characteristic size of a dense core in the Taurus molecular cloud which forms only one, or at most a handful of stars. The clusters IC 348, NGC 2024, and the Trapezium contain approximately 30, 50 and 100 stars in their central 0.1 pc regions. The implied stellar mass and equivalent molecular cloud densities of these clusters, correcting for projection effects (McCaughrean & Stauffer 1994), range from 2.5 - 8.2 x 10^3 $M_\odot$ pc^{-3} and 5-16 x 10^4 cm^{-3} respectively for the three clusters (Lada & Lada 1995). The latter range of densities is consistent with the range of molecular hydrogen densities measured on similar spatial scales in the densest regions of massive cluster forming cores (Lada, Evans & Falgarone 1997). If such high stellar densities were characteristic of those at formation, then this would have important consequences for star formation theory and our understanding of protostars. However, it is possible that the observed stellar densities do not reflect the initial cluster densities given that the dynamical time scales of such clusters are much shorter than their ages. Therefore it is possible

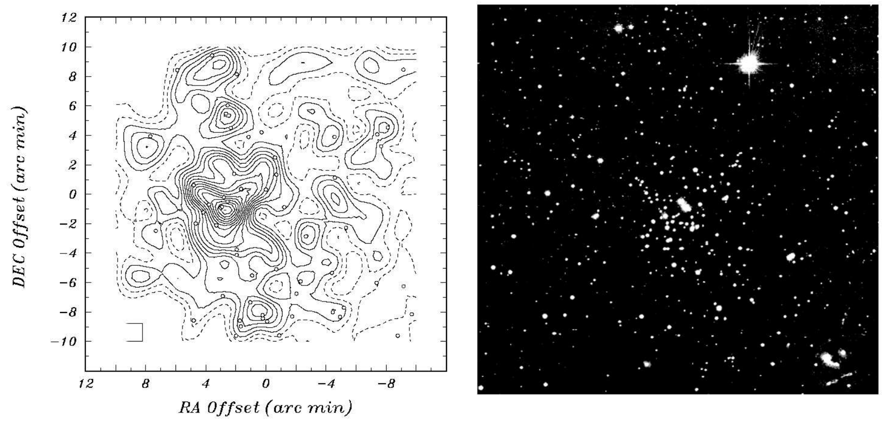

Figure 10. A K-Band image of the IC 348 cluster, located in the Perseus molecular cloud is shown on the left. A contour map of the stellar surface density as measured at K is shown on the right. (Lada & Lada 1995). Open circles represent the distribution of near-IR excess sources. See text for more details.

that the stars have evolved to denser configurations than they started out with (Lada Margulis & Dearborn 1984; Patel & Pudritz 1994).

Finally, the inferred volume mass densities of young embedded cluster are at least two orders of magnitude greater than that of optically visible open clusters such as the Pleiades (Lada & Lada 1995). This large disparity is consistent with the predictions of models for the dynamical evolution of young clusters that form in molecular clouds with low star formation efficiencies (e.g. Lada et al. 1984).

3.3. THE BINARY FRACTION IN YOUNG CLUSTERS

It is well known that a large fraction ($\sim$ 50%) of stars in the Galaxy are members of binary, rather than single star systems (Abt 1983; Duquennoy & Mayor 1991). Therefore, it is not too surprising that surveys of pre-main sequence (PMS) stars in isolated nearby star forming regions, such as Taurus, have revealed that even stars in the earliest stages of stellar evolution are also found in binaries. In fact, binaries are found even among the very youngest PMS stars located near the stellar birthline in the HR diagram. This indicates that binary formation occurs as a direct consequence of the star formation process, e.g. binaries form in the protostellar phase, rather than the PMS stage of stellar evolution at least in low density regions. At the same time, however, such studies have suggested that PMS stars have a significantly higher companion frequency than main sequence stars in the separation ranges studies (i.e. 2-3 times higher than the field) (Ghez et al.

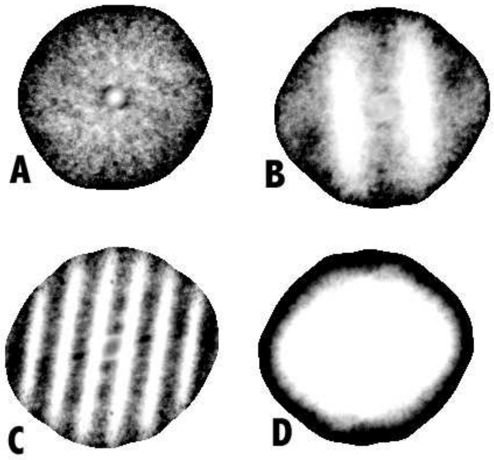

Figure 11. Calibrated power spectra for stars in the NGC 2024 young embedded star cluster obtained with NIRC on Keck I. Panel A shows an essentially unresolved object. Panel B hows a binary with a separation of $0.09''$. Panel C shows a binary with a $0.35''$separation. Finally, Panel D shows a single star with a luminous resolved envelope or circumstellar disk.

1993; Leinert et al. 1993; Reipurth & Zinnecker 1993; Simon et al. 1995). One implication of these findings is that stellar binarity may be more common in the earlier PMS stages of evolution than during the main sequence phase. If this is true then many binary systems must somehow be disrupted during the course of their PMS evolution.

Searches for binary stars in clusters such as the Pleiades (Bovier et al. 1997), IC 348 (Duchene et al. 1998) and the dense Trapezium cluster (Petr et al. 1998; Prosser et al. 1994) have revealed binary fractions in these clusters similar to that of the field. These findings reinforce the idea that most stars in our Galaxy form in clusters and not isolation. Recently, Lada and Elston (1999) obtained near-IR speckle observations of 43 stars in the NGC 2024 cluster using Keck I. Figure 11 shows the calibrated power spectra for a sample of stars observed. We found 12 of the 43 stars observed to be binaries in the separation range from 0.05 arc seconds to 1 arc second. This leads to a binary fraction in NGC 2024 of 28±8%, but the true fraction is slightly higher since the data have not yet been corrected for missed binaries with small separations and large magnitude differences. This binary frequency is very similar to the high binary frequency found in Taurus over the same physical separation range (32 ± 3%). However, given the large statistical uncertainty, it is also consistent with the expected binary fraction for G-dwarf field stars in the same physical separation range (19 ± 3%) and a better statistical sample is needed before we can differentiate between the Taurus fraction and the field. These new observations of the very young NGC 2024 cluster, while not definitive, leave open the possibility that binaries form with the same frequency whether they form in clusters or in isolation. If so, then binaries formed in clusters are quickly disrupted whereas binaries formed in isolation survive for longer periods of time. Again this picture would be consistent with observation that most stars form in embedded clusters, which later disperse to populate the field.

3.4. NEAR-INFRARED LUMINOSITY FUNCTIONS

Young embedded clusters offer unique opportunities to study the stellar initial mass functions (IMF) and its possible variation in space and time. Such clusters are not old enough to have lost significant numbers of members due to stellar evolution or dynamical effects. In addition, mass segregation is not as big a problem as in classical open clusters. The biggest advantage of using very young clusters for studies of the initial luminosity function is that the low mass stars in these clusters are brighter than at any other time in their pre-main sequence evolution. Consequently modern near-IR detectors even on modest telescopes can completely sample the entire IMF of nearby (D < 1Kpc) embedded clusters down to the hydrogen burning limit. The high stellar surface densities in young clusters combined with the high luminosities of the low mass stars also makes issues of membership determination much less of a concern than in older open clusters. Embedded clusters are rich (N>100 stars) and provide statistically significant samplings of the IMF at virtually all masses. However there are also disadvantages to studying young embedded clusters. First the youngest stars in clusters are still heavily embedded in their parental gas and dust. Consequently, the extinction toward cluster members can be highly non-uniform even at infrared wavelengths. In addition, due do the youth of the clusters, most members are still in the pre-main sequence phase of their evolution. Since there is no unique mass to luminosity relation for pre-main sequence stars, one must rely on using evolutionary models. Finally, because the clusters are young, many of the stars exhibit excess near-IR emission above their photospheric emission due to the presence of circumstellar dust or protostellar envelopes.

Comparison of the K-band luminosity functions or KLFs for such nearby young clusters has shown that these KLFs often exhibit two general characteristics. First, the shape of a cluster KLF often approximates a power-law for the brightest stars. Second, the KLF departs from this power-law, flattening out and turning over at the faintest magnitudes. An example of such a KLF is shown in Figure 12 for the IC 348 cluster. IC 348 is a relatively rich and young cluster located in the Perseus molecular cloud at a distance of 320 pc. In the top panel of Figure 12, the KLF for all stars observed toward the cluster is plotted as a histogram, as well as the KLF for stars in a nearby, equal sized, off or control field. The control field stars were artificially extincted by 0.5 magnitudes at K to approximately account for the extinction due to the associated molecular cloud. The shape of the KLF for the stars observed toward the cluster is somewhat different than that off the cluster. In the off field KLF, the number of sources increases with increasing K magnitude up to the completeness limits of our observations ($m_K = 14$). In contrast, the number of sources in the cluster KLF increases with increasing K magnitude until $m_K \sim 11$ after which the number of sources levels off and and then turns over near the completeness limit. The bottom panel shows the IC 348 KLF resulting from the subtraction of the KLFs of the cluster and extincted control field. This differential KLF represents the luminosity function of the cluster members. The slope of the power-law portion of the KLF is equal to 0.40 (± 0.03), similar to the slopes of the power-law portions of the KLFs of other young clusters. The IC 348 KLF departs from the power-law for fainter stars, flattening out at around $m_K \sim 11$ magnitude.

While the KLFs of most nearby clusters share these 2 general features, direct comparison of individual clusters shows that their KLFs can also differ significantly. In particular, both the widths of the KLFs and the points of departure from a power-law can differ from one cluster to another. For example, the KLFs for the Trapezium and NGC 1333 clusters are significantly narrower than that of IC 348 (see Figure 13) (Lada, Alves & Lada 1996).

In principle, the luminosity functions of young embedded clusters should provide fundamental constraints on issues concerning the IMF. Various groups have modeled the luminosity functions of young clusters using realistic stellar mass functions and appropriate mass-luminosity relationships (Zinnecker et al. 1993; Fletcher & Stahler 1994a, b; Megeath 1996; Lada & Lada 1995; Muench, Lada & Lada 1999). From a comparative analysis of published observations of the Trapezium cluster with such KLF models and observations of IC 348, Lada & Lada (1995) concluded that the underlying mass function of both clusters is similar to the IMF for field stars down to the hydrogen burning limit. In addition they found little evidence for a significant population of single, lower mass objects (brown dwarfs). Further comparisons of the KLFs of the young NGC 1333 cluster with IC 348 and the Trapezium show that the shape of the KLF of NGC 1333 is similar to that of the Trapezium but that both differ from the KLF of the older IC

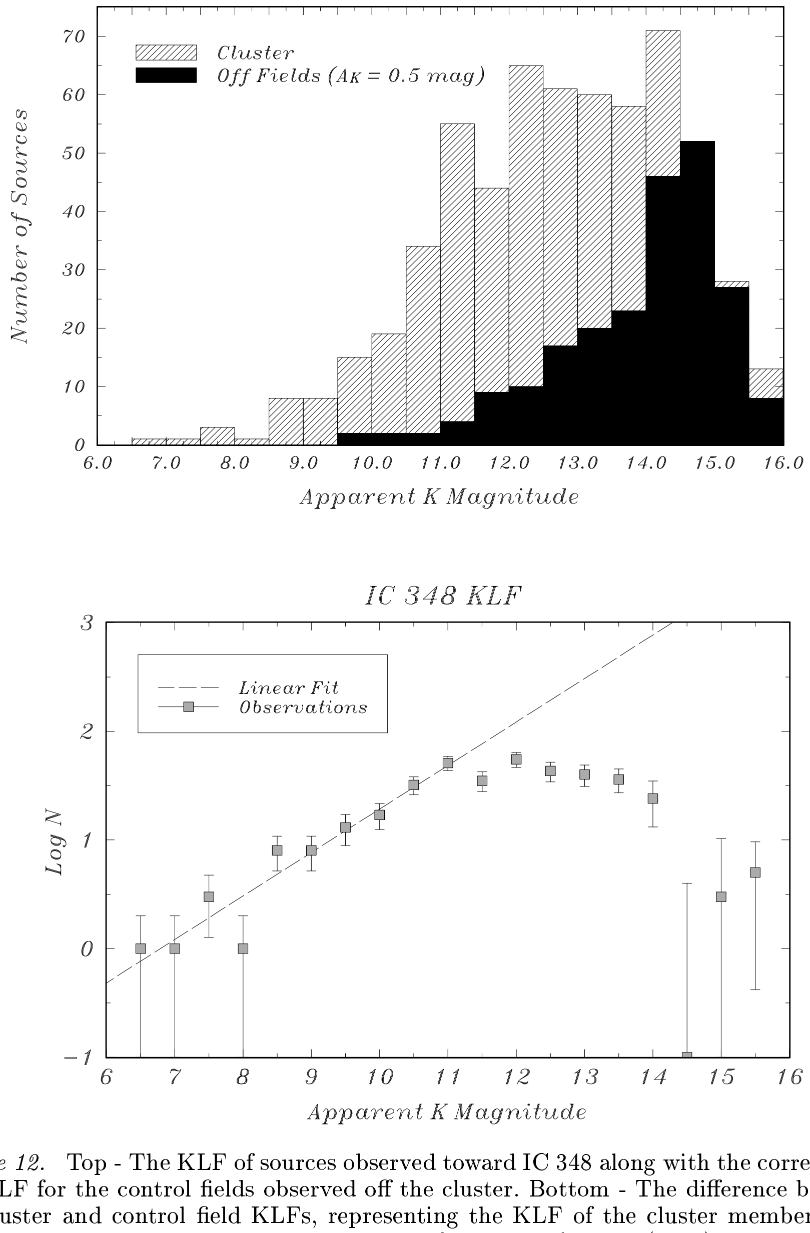

Figure 12. Top - The KLF of sources observed toward IC 348 along with the corresponding KLF for the control fields observed off the cluster. Bottom - The difference between the cluster and control field KLFs, representing the KLF of the cluster members. The source counts are complete to m_K=14. Taken from Lada & Lada (1995).

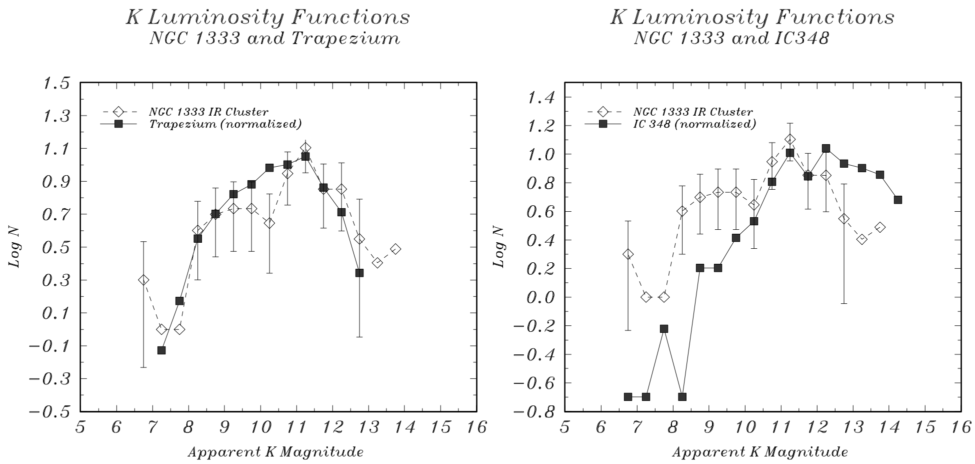

Figure 13. This figure from Lada, Alves & Lada (1996) compares the observed KLFs for three nearby young clusters: the Trapezium in Orion, NGC 1333 and IC 348 both in Perseus. The KLFs of the Trapezium and IC 348 clusters have been normalized to the size of the population of the NGC 1333 cluster. Additionally, the KLF of the Trapezium has been corrected to the distance modulus of NGC 1333, which we have taken to be the same as for IC 348 (m-M=7.5).

348 (Lada, Alves & Lada 1996). This can be attributed to the affects of luminosity evolution and suggests that the age of NGC 1333 is similar to that of the Trapezium but is significantly less than that of IC 348. For a more comprehensive review of young cluster luminosity functions and their interpretation with regards to issues concerning the IMF, the reader is referred to a review by Lada et al. (1998) and the chapter by C. Lada, this volume.

Despite the similarities in their mass functions, embedded clusters appear to be characterized by significantly different rates of star formation over their lifetimes. For example, the rate of star formation in the Trapezium has been more than 10 times greater than that in NGC 1333 and IC 348 (Lada & Lada 1995; Lada, Alves & Lada 1996). The difference in the star formation rates in these clusters suggests that the star formation mechanism can be very sensitive to initial conditions. It is possible that differences in environment (O stars in the Trapezium versus no O stars in either IC 348 or NGC 1333), could be responsible for the differing rates. However, evolutionary modeling of more clusters is needed to be able to test this or any hypothesis concerning the origin of the differing star formation rates observed in clusters.

4. The Formation of Embedded Clusters

Comparisons of the location of embedded clusters with the distribution of dense gas in L1630 (Lada 1992) (Figure 14) indicate that the young clusters are associated with and most likely formed from the most massive dense cores in the cloud. Similar results have been found in the Gem OB1 molecular cloud (Carpenter et al. 1995) and also the Rosette molecular cloud (Phelps & Lada 1997). Therefore, in order to understand how an embedded cluster forms, we must understand two basic physical processes: (1.) the formation of a massive, dense molecular core in a molecular cloud and (2.) the subsequent development of stars from the dense gas in the core (see chapters by Bonnell, McKee and Myers). Studies of molecular cloud structure provide insights into some important aspects of embedded cluster formation. For example, the slope of the mass spectrum of dense cores derived from the CS survey of the L1630 cloud indicates that a substantial fraction of the mass of dense gas is contained within the most massive dense cores (Lada, Bally, & Stark 1991; see Chapter by C. Lada, Figure 6). Consequently the observation, that the majority of the star formation in L1630 has occurred in clusters, may be naturally explained to a large extent by the fact that most of the dense gas in the cloud is contained within a few localized and massive, dense cores. Furthermore, investigations of the structure of other nearby clouds have strongly suggested that the mass spectra for clumps and cores in GMCs is universal (Blitz, 1993; see Chapter by Blitz). For example, Kramer et al. (1998) recently derived the mass spectra for seven molecular clouds (Figure 15) and found that mass spectra were consistent with a powerlaw, $dN/dM \propto \; M^{-\alpha}$, where $\alpha \sim 1.7$, similar to the mass spectra measured in other clouds and for the dense gas in L1630. This suggests that GMCs, in general, should produce most of their stars in embedded clusters.

Comparison of surveys for dense molecular gas and for young stars in GMCs can provide us with many insights into the star forming process in molecular clouds. Such surveys in the L1630 cloud have demonstrated that (1.) star formation within this cloud occurs almost exclusively within the dense ($> 10^4$ cm^{-3}) gas, and that (2.) star formation does not occur uniformly throughout the dense gas but is strongly favored in a few very massive (M$>$200M$_\odot$) dense cores, where the efficient conversion of molecular gas into stars has resulted in the production of rich stellar clusters (Figure 14). The three massive cores, NGC 2071, NGC 2068 and NGC 2024, associated with the rich embedded clusters in L1630 account for $\sim$ 30% of the total mass of dense gas in the cloud but only 8% of the total molecular cloud mass, suggesting that only a small fraction of a GMC has the conditions needed for efficient star formation.

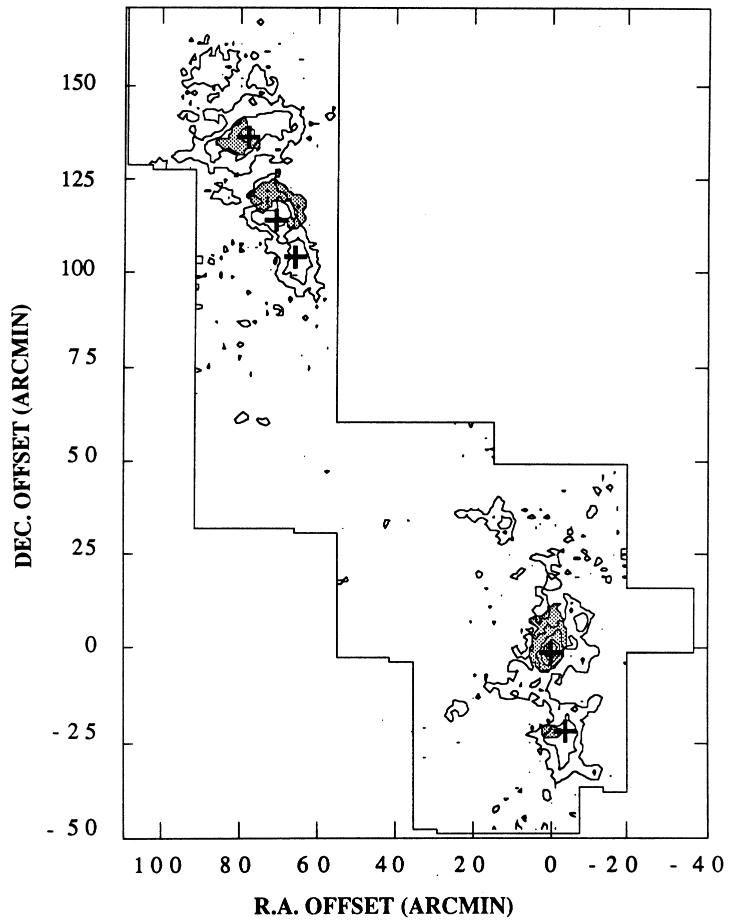

Figure 14. Comparison of embedded cluster locations and the distribution of dense gas in the L1630 molecular cloud. The shaded regions represent the location and extents of the embedded clusters. The contours show the map of CS(2-1) integrated intensity in the velocity range of 7-13 km s^{-1}. The (0,0) position is the same as in Figure 5. The lowest CS contour level is at 0.8 K km s^{-1}, which corresponds to a 3 sigma level detection. In addition the locations of the five most massive CS cores identified by Lada, Bally & Stark (1991) are represented by large crosses. The solid line represents the boundary of the CS survey.

While the observations of L1630 confirm the idea that clusters form from massive dense cores, they also suggest that high mass and high density may not be sufficient conditions for cluster formation. In addition to the massive cluster-forming cores, the L1630 cloud was found to contain a massive, dense core, LBS 23, that is not associated with a recognizable cluster. This core is however associated with current star formation (e.g. Bontemps et

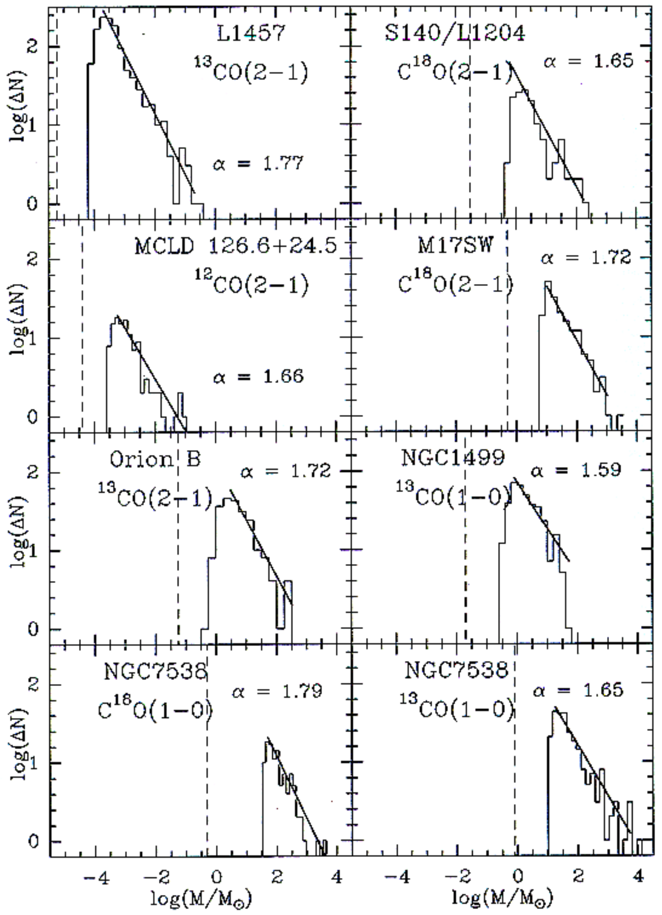

Figure 15. The clump mass spectra for seven molecular clouds measured by Kramer et al. (1998). The slopes of these spectra are consistent with previous measurement of mass spectra of other nearby GMCs (e.g. Blitz, 1993) and the mass spectrum determined for the dense cores from CS observations of the L1630 molecular cloud (Lada, Bally & Stark, 1991).

al. 1995). In addition, another massive core, NGC 2023 was found to contain only a very poor cluster. In these two massive cores the level of star formation is much lower than in the three other cores of comparable mass that are producing rich clusters. This difference is reflected in estimates of the star formation efficiencies (SFEs) of these cores. Assuming an average or typical stellar mass of 0.6 $M_\odot$ for stars in the embedded clusters, Lada, Evans & Falgarone (1997) derived SFEs (SFE = $M_{stars}/M_{stars+gas}$) for the cores from the total number of stars in each cluster and the mass of the gas in each core (Lada 1992). As a result, the NGC 2071, NGC 2068 and NGC 2024 cores have star formation efficiencies on the order of 10% – 30%, whereas the LBS 23 and NGC 2023 cores exhibit SFEs $\sim$ 4%. The vast differences in the star formation activity in the five massive CS cores in L1630 could be due to either differences in the fundamental physical properties of the cores or differences in evolution.

In order to determine whether the physical properties of massive cores are related to their star formation efficiencies and, in particular their ability to form rich embedded clusters, the spatial and density structure of the massive cores and two low mass cores in L1630 were examined using multi-transition CS observations of the cores with spatial resolutions ranging from $11'' - 64''$(Lada, Evans, Falgarone 1997). The data were analyzed using an LVG model. Densities at least as high as 10^5 cm^{-3} were found to exist in all the massive cores. Comparison of the properties of massive cores with and without an associated embedded cluster reveal that cores having high SFE and consequently forming rich embedded clusters, tend to have larger regions of high density gas (i.e. have larger areas of detectable CS (J=5-4) emission) than those having low SFE and not associated with a populous cluster. In addition, the filling factor of gas at densities above 10^5 cm^{-3} is smaller for cores forming rich clusters than for the others. These differences suggest that regions forming rich embedded clusters require a large fraction of their gas to have densities exceeding 10^5 cm^{-3}, and that they are more fragmented. In contrast, regions with small amounts of dense gas and high volume filling factor (less fragmented) seem to produce only small numbers of stars.

5. Fate of Embedded clusters

It is interesting to note that Roberts (1957) estimated that only 10% of all stars born in the galaxy formed in exposed clusters. This is roughly an order of magnitude lower than the estimate of the fraction of all stars formed in embedded clusters in the Orion clouds. Are the Orion clouds unusual in their cluster forming properties or do embedded clusters rarely form bound systems. The key to answering this question involves understanding the physical association of the clusters with the interstellar gas that they are embedded in.

The dynamical evolution of embedded clusters and their emergence from molecular clouds has been well studied both analytically (e.g. Hills 1980; Mathieu 1983; Elmegreen 1983; Elmegreen & Clemens 1985; Verschueren & David 1989; Verschueren 1990; Saiyadpour et al. 1997) and numerically (Lada, Margulis & Dearborn 1984; Kroupa 1995) and is also discussed in Lada & Lada 1991. As already discussed, embedded clusters form in dense, massive molecular cloud cores. These systems are strongly gravitationally bound systems, as seen from their high mass densities and moderate internal velocity dispersions. However, as we have seen, the star formation efficiency in these systems is relatively low (10% - 30%) and consequently a large fraction of gravitational binding energy for the system is provided by the gas. As long as the star formation efficiency is not very high, the evolution of the cluster depends sensitively on the evolution of the gas.

Molecular outflows, stellar winds and HII regions from the more massive stars in embedded clusters can violently disrupt the molecular gas in a dense core on time scales which are shorter than or comparable to the dynamical time of the system. When this occurs, the dynamical response of the stars which are left behind will depend primarily on the star formation efficiency achieved in the core at the moment of dispersal. In the face of rapid gas removal, a bound group will only emerge if the star formation efficiency is $> 50\%$ (i.e. Lada et al. 1984). Given the low star formation efficiencies of the known embedded clusters, such as the L1630 clusters, it is not too difficult to account for the low fraction of stars born in bound visible clusters. It is likely that most embedded clusters emerge from molecular clouds as unbound systems. Thus, although most stars may form in rich embedded clusters, these stellar groups evolve to become the cores of unbound associations, not bound open clusters.

6. Circumstellar Disks in Cluster Environments

The recent detections of extra-solar planets are among the most exciting and significant discoveries of the 20th century. Their discover has sparked intense interest in two of the most fundamental unsolved mysteries in modern astrophysics: (1.) how common are extra-solar planets in the Galaxy? (2.) what are the origins of planetary systems? Theoretical considerations suggest that a natural consequence of the collapse of a rotating gas cloud is the formation of a protostar with a surrounding accretion disk (Shu et al. 1993; see chapter by Ruden). It is within such disks that planets are thought to form. Over the past ten years, observers have assembled compelling evidence supporting this scenario: namely that circumstellar disks frequently exist around young stellar systems. This evidence has been based mainly on the unique emission characteristics of the disks at infrared and millimeter wavelengths (Shu et al. 1993; Welch & Sargent 1993; Lada, 1991). The evidence for proto-planetary systems rests largely upon assessments of the masses in disks (e.g. Beckwith & Sargent 1991, 1993) and the rate at which these masses evolve (Skrutski et al. 1990).

Most of our knowledge of young circumstellar disks has been derived mainly from considerations of isolated star systems in regions where stellar densities are low (e.g. Taurus). However, as we have already discussed, most stars are probably born in dense embedded clusters and not in isolated protostellar fragments. The natal environment of a massive core, which is forming a cluster, should be quite different than that of a low mass core producing only one or two isolated new stars and one might expect to find fundamental differences in the physics of the star forming process between such regions. For example, the dense stellar environments of the young clusters may influence the formation and lifetimes of disks around the newly formed cluster members and consequently influence planet formation. Indeed numerical simulations suggest that the disk lifetimes may be significantly shortened in dense clusters (Clark & Pringle 1991; Larson 1990). Given that a significant fraction of stars in the Galaxy form in clusters, establishing the properties of disks in crowded environments is essential to our understanding of the overall likelihood of planetary systems in the Galaxy.

In regions of star formation, one expects to find young stellar objects in differing stages of evolution, from protostars to pre-main sequence stars. In order to study the natures of circumstellar disks in clusters, we must be able to distinguish between the different evolutionary phases of young stellar objects in the clusters and identify those sources with disks. Since young stellar objects are associated with large amounts of gas and dust, they radiate a significant fraction of their energy at infrared wavelengths and consequently their infrared spectral energy distributions should reflect the nature and distribution of the material surrounding them and their evolutionary state (Lada 1987; Adams, Lada and Shu 1987). It has been demonstrated that YSOs can be meaningfully classified into at least three distinct classes based on the shapes of their broad band (1-100 μm) energy distributions (Lada and Wilking 1984; Adams, Lada and Shu 1987; Myers et al. 1987). These classes represent an evolutionary sequence of YSOs from protostar to young main sequence star (Lada 1987; Adams, Lada and Shu 1987). Class I sources have strong 'infrared excesses' (i.e. infrared energy distributions that are broader than a blackbody distribution) and their spectral energy distributions are characterized by positive slopes at wavelengths longer than 2 μm. Class I sources are likely protostellar in nature (Adams and Shu 1986; Adams, Lada and Shu 1987). Class II sources also have infrared excesses, but their energy distributions are characterized by flat or decreasing slopes at wavelengths longer than 2 μm. They are surrounded by considerably less circumstellar material than protostellar objects and their infrared excess is thought to arise in circumstellar disks (Rucinski 1985; Adams, Lada and Shu 1987; Kenyon and Hartmann 1987; Rydgren and Zak 1987; Strom et al. 1988). Class III objects have little or no infrared excess emission and their energy distributions are characterized by reddened blackbody functions. These sources are also optically visible and include young main sequence stars and also younger pre-main sequence stars that no longer have optically thick circumstellar disks such as the weak-lined or naked T Tauri stars (e.g. Walter 1987).

6.1. NEAR-INFRARED STUDIES OF CIRCUMSTELLAR DISKS

Ideally, one would like to obtain broad band energy distributions of significant numbers of embedded cluster members in order to study the frequency and lifetimes of the protostellar and disk phase of evolution. This is a difficult proposition given the current detector technology at longer wavelengths. Fortunately, Lada & Adams (1992) have shown that protostellar sources, AeBe stars and the majority of T Tauri stars are characterized by JHK infrared colors which place them in the infrared excess region of the JHK color-color diagram. Figure 16 shows a JHK color-color diagram for YSOs in Taurus. In this figure the locus of the main sequence is represented as a solid line and the region encompassing reddened main sequence stars is enclosed by the dotted lines. Stars that fall to the right of these reddening lines have an infrared excess. While not completely unambiguous, protostars (Class I), classical T-Tauri stars (ClassII and Weak-lined T-Tauri stars (class III) do separate, occupying differing regions of the color-color diagram. Further a large fraction ($\sim$ 50%) of Class II sources lie in the near-IR excess region.

An analysis of the infrared colors for several young clusters has been made and the results are presented in Table 2. For many clusters, a large fraction of the cluster sources exhibit significant near infrared excess indicating the possible presence of a circumstellar, proto-planetary disk. Typically, only half the stars with such disks exhibit measurable near-IR excess emission. The high fraction of excess sources in clusters such as NGC 2024, NGC 1333, Rho Oph, etc., suggests that there is a high fraction (100%) of protostellar sources or sources with disks in these young clusters. This is quite remarkable, given the high stellar densities in the cluster cores (i.e. Table 1). In contrast, a number of clusters, such as IC 348 and NGC 2362, have a small detectable near infrared excess fraction. This is consistent with these clusters being older. Figure 17 plots the near-IR excess fraction of young clusters versus their estimated age. The fraction of near-IR excess sources clearly decreases with increasing age and from this we estimate the lifetime of disks in such environments to be only a few million years. The comparison of the fraction of near-infrared excess sources in clusters of differing age, illustrates the potential power of using the infrared energy distributions of YSOs in clusters to constrain the timescale for the disk phase of stellar evolution.

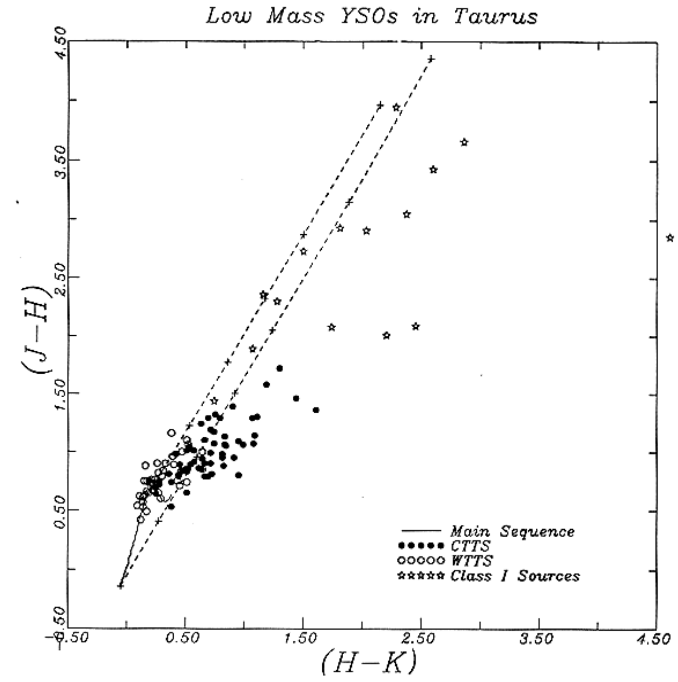

Figure 16. The JHK color-color diagram for low-mass YSOs in the Taurus-Auriga dark cloud complex. The figure is taken from Adams & Lada (1992) and the data were taken from Kenyon & Hartmann (1995). See text for a description of the figure.

Near-IR Excess Fraction in Clusters

Cluster	Excess Fraction	Reference
IC348	20%	Lada & Lada 1995
NGC 1333	60%	Lada, Alves & Lada 1996
NGC 2024	>60%	Comeron et al. 1996
		Lada et al. 1999
NGC 2068	38%	Lada,& Dahari 1999
NGC 2071	34%	Lada, & Dahari 1999
Trapezium	>50%	McCaughren & Stauffer 1996
		Hillenbrand et al. 1998
ρ Oph	50-70%	Green & Young 1992
		Strom, Kepner & Strom 1995
R Mon	62%	Carpenter et al. 1998
NGC 2362	0%	Alves et al. 1999

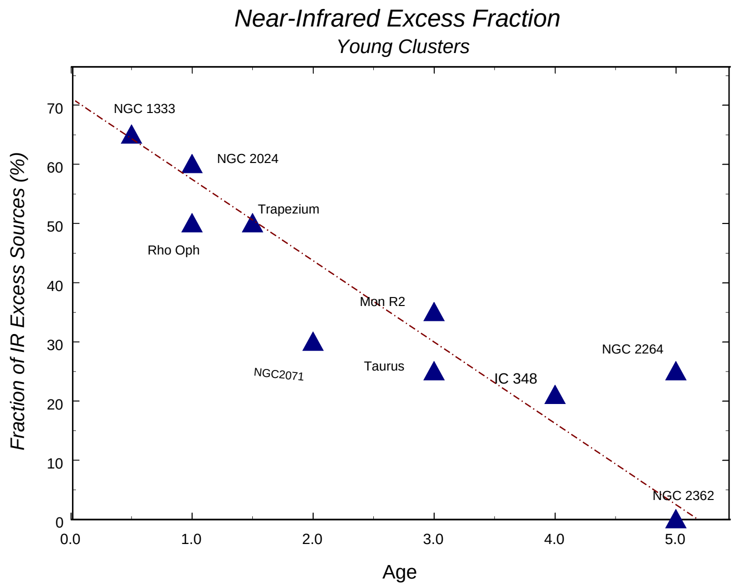

Figure 17. The fraction of near-infrared excess sources in embedded clusters as a function of cluster age. The near-IR excess fraction decreases with increasing cluster age, suggesting estimates of the lifetime of circumstellar disks on the order of a few million years.

Near infrared observations by themselves, however, are of limited use in investigating the evolutionary status of young stellar objects in clusters because of the complications introduced by extinction and scattering. In addition these wavelengths are still not long enough to avoid significant contamination from normal stellar photospheric emission. Consequently, the near-infrared observations are capable of identifying only sources with relatively strong infrared excess and this accounts for only about half of the sources which actually possess circumstellar disks. For example, in the NGC 2024 cluster (Figure 18), it is not clear whether the large number of near-IR excess sources is due to the presence of disks, protostellar envelopes, or caused by emission nebulosity due to the HII region. Therefore such observations cannot distinguish between Class I, Class II and Class III sources especially in regions of high extinction. Combining near-infrared observations with longer wavelength (e.g. 3-20 μm) observations can help alleviate some of this ambiguity (Figure 19). Since contamination from photospheric emission is minimal at mid-infrared wavelengths, the presence of circumstellar, proto-planetary disks can be ascertained from observations

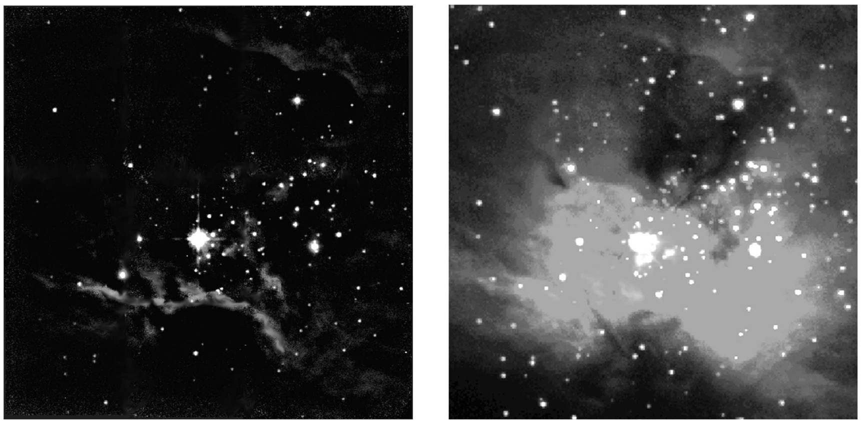

Figure 18. Near-Infrared images of the NGC 2024 embedded cluster. On the left is an L band image taken with the SAOIRCAM on the 48 inch telescope at Mt Hopkins. On the right is a K-Band image taken with SQIID on the 50 inch telescope at Kitt Peak. The images cover $\sim$ 20 $\times$ 20 arcmin region on the sky.

of 10 μm with little ambiguity if near-infrared data is also available. For his thesis, Karl Haisch is conducting an L-Band and mid-IR survey of a sample of young clusters to determine a more robust estimate of the disk fraction as a function of age in cluster environments. Recently obtained L-band and mid-IR images of the NGC 2024 region (Figure 18) confirm a large fraction of disk sources within this dense young cluster (Haisch, Lada, & Lada, 1999; Haisch, Lada & Pina 1999). An analysis of the JHK and L colors for the brightest young sources in NGC 2024 indicate a disk fraction of $\sim$ 60%. Furthermore, out of the 60 near-IR sources surveyed, approximately 60% exhibit 10 micron emission. This fraction is consistent with the fraction of near-IR (JHK) excess sources seen in the cluster (Comeron, Rieke & Rieke 1996; Lada & Dahari 1999).

6.2. MILLIMETER CONTINUUM OBSERVATIONS OF CIRCUMSTELLAR DISKS AND DISK MASSES

While near-infrared and mid-infrared data are essential for identifying sources having circumstellar disks, they are inadequate for determining the masses of the disks. Knowledge of disk masses is key for determining whether or not circumstellar disks can form planets. In almost all cases, disk masses can be estimated only from the dust continuum emission at millimeter wavelengths, where the dust is optically thin (e.g. chapter by Beckwith). An excellent place to investigate the formation and survival of circumstel-

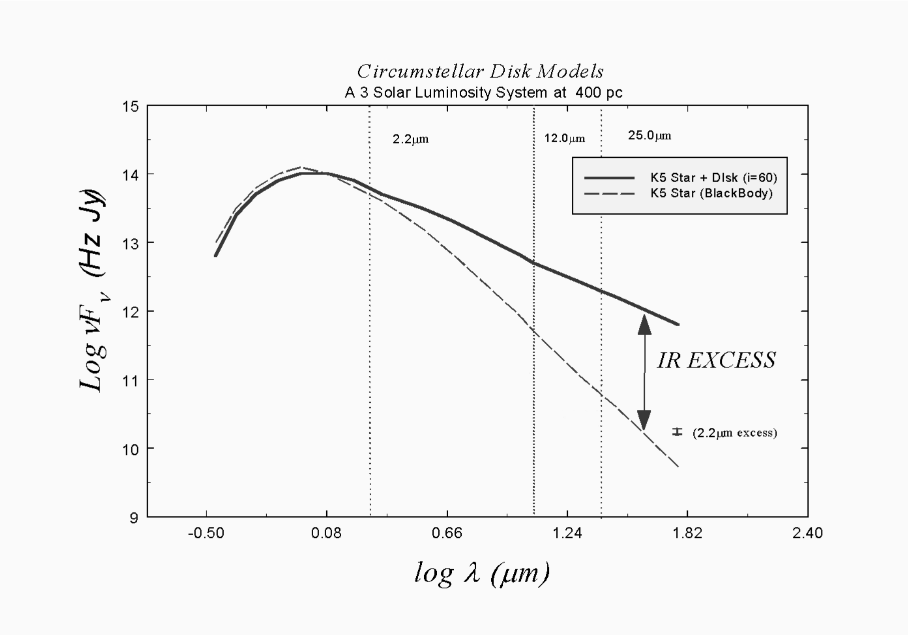

Figure 19. A model of the spectral energy distribution for a 3 solar luminosity disk plus star system at 400 pc (solid line). The stellar black body distribution is plotted for comparison (dashed-line). This figure illustrates the advantage of observations longward of 2 microns for surveys for emission from circumstellar disks.

lar disks in cluster environments is the Trapezium cluster. Located in the Orion molecular cloud complex, it is one of the nearest (D $\sim$ 440 pc), rich, young clusters. The Trapezium has an age of $\sim$ 1Myr and exhibits stellar densities of $5\times\ 10^4$ stars per pc^{-3} in its core (see Table 1). Strong evidence for the existence of circumstellar disks in the Trapezium come from centimeter emission (Churchwell et al. 1987; Garay, Moran & Reid 1987; Felli et al. 1993), near-IR excess (McCaughrean & Stauffer 1994) and HST observations of disks in emission (proplyds) and absorption (O'Dell, Wen & Hu 1993; O'Dell & Wen 1994). First attempts to detect millimeter continuum emission from circumstellar disks in the Trapezium and estimate their masses were carried out using the BIMA interferometer (Mundy, Looney & Lada 1995). While these observations sampled a large area of the cluster (4-8 arcmin^2), they were not sensitive enough to place strong constraints on disk masses. Only upper limits of $< 0.15\ M_{\odot}$could be placed on the masses of individual disk systems identified by O'Dell and Wen (1994) in the vicinity of Theta 1 C. This limit is larger than the typical disk masses measured in the Taurus region. In order to obtain a meaningful census of disk masses in the Trapezium cluster, more sensitive observations are required.

Using the IRAM interferometer, Lada et al. (1999) have obtained sensitive 1.3 mm and 2.7 mm continuum observations of 2 fields in the Trapezium cluster containing 34 near-IR sources and 20 proplyds. The sensitivity of these observations permits the detection (at 4 sigma) of disks with masses 0.005 $M_\odot$, more than an order of magnitude smaller than previous interferometer observations of this cluster and sufficiently sensitive to detect the minimum mass solar nebula. These observations resulted in the *first* 1.3 mm continuum detections of circumstellar disk material associated with the near-IR sources and proplyds in the extreme environment of the Trapezium cluster and provide the first estimates of disk masses in this cluster. Three sources, HST 170-337, 171-340 and 158-327 were detected at approximately the 10 sigma level (Figure 20). The sources have 1.3 mm fluxes ranging from 9.9 to 11.3 mJy. The three detections are coincident with known proplyds and near-infrared sources. Disk masses were estimated in two ways: (1.) by comparing the measured fluxes for the Trapezium sources to the mm flux measured for HL Tau, which has a well established disk mass of 0.1 $M_\odot$ (Beckwith and Sargent 1991) and (2.) by assuming the dust is optically thin and adopting standard assumptions about the dust mass opacity, temperature and mass distributions (see chapter by Beckwith for a detailed discussion of how to calculate disk masses). Using either method, the disk masses for the three Trapezium detections were estimated to be on the order of 0.01 $M_\odot$. This is more than an order of magnitude smaller than HL Tau, the most massive disk in Taurus and comparable in mass to the minimum mass solar nebula.

Surprisingly, *only* 3 sources, coincident with previously identified proplyd and near-IR sources, were detected in this study. The area of the Trapezium cluster surveyed with the IRAM interferometer contained ~ 20 identified proplyds and ~ 34 identified near-infrared sources. This leads to disk detection rates of 15% for the proplyd sources and only 10% for the near-infrared sources. These disk detection rates are much lower than the detection rates measured by near-infrared excess ($> 50\%$), for the inner portions of the disks around young stars in this cluster (i.e. Table 2).

As part of a complementary survey for 1.3 mm emission from circumstellar disks in clusters, Lada & Beckwith (1999) surveyed approximately 48 near-infrared sources in the NGC 2071 cluster in L1630 for 1.3 mm continuum emission from disks, using the 19 element bolometer array on the IRAM 30 m telescope. As a result, 22 out of the 48 sources were detected at a > 3 sigma level. Most of the sources detected were compact and detected only in 1 beam of the array. Follow up observations of several detections have recently been carried out with the IRAM interferometer to confirm that the millimeter emission is coming from a disk rather than

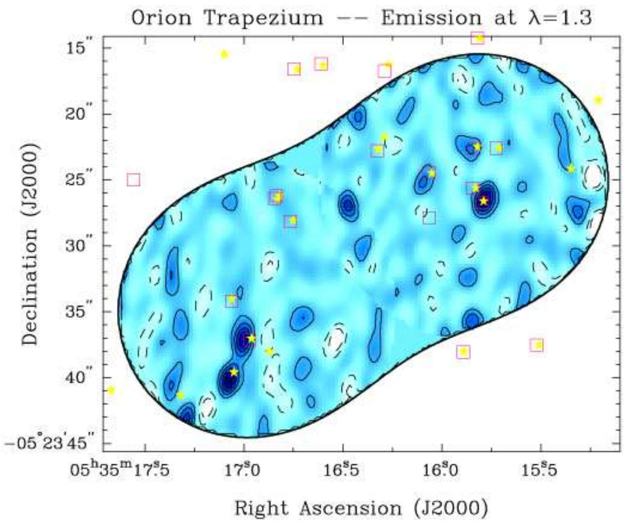

Figure 20. The first detection of dust continuum emission from the Orion proplyds. A contour map of 1.3 mm continuum emission of a region in the Trapezium cluster is presented. The data were taken with the IRAM interferometer (Lada et al. 1999)

from extended emission around the source (Haisch & Lada 1999). It is notable that the detection rate of 1.3 mm continuum sources in NGC 2071 (46%) is much higher than the rate found in the Trapezium cluster (10%), even though the two clusters have comparable ages and NGC 2071 has a lower fraction of near-infrared excess sources than the Trapezium. Since NGC 2071, unlike the Trapezium, does not contain any O stars this suggests that the presence of O stars in a cluster may significantly affect the lifetimes of disks in clusters.

The distribution of 1.3 mm flux for the young NGC 2071 cluster, is similar in range, down to the detection limits, to the distribution in Taurus (Beckwith et al. 1990; Osterloh & Beckwith 1995), corrected for distance (Figure 21). However, at least two sources in NGC 2071 have higher 1.3 mm fluxes than in Taurus. These results suggest that the range of disk masses in the NGC 2071 cluster may be similar to the more isolated Taurus environment.

Figure 21 also compares the distribution of 1.3 mm continuum fluxes for the detected Trapezium sources with the distributions for NGC 2071 and

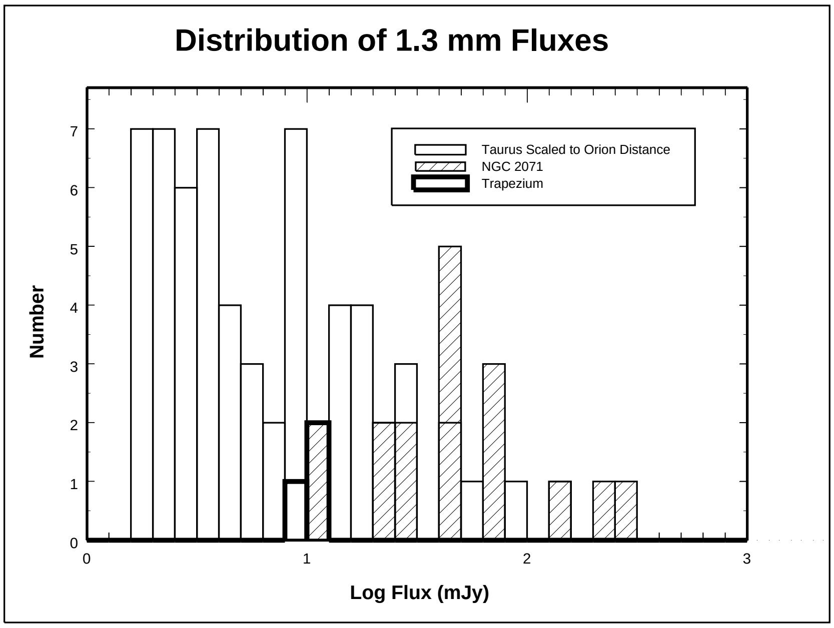

Figure 21. A comparison of the distribution of 1.3 mm continuum fluxes for sources in Taurus, the NGC 2071 cluster and the Trapezium cluster is presented. The fluxes for the Taurus sources were taken from Beckwith et al. (1990) and have been scale to the distance of Orion.

Taurus (corrected for distance to Orion). The largest fluxes measured for the Trapezium sources are an order of magnitude smaller than the largest fluxes measured for sources in NGC 2071 or Taurus. Remember that the majority of near-infrared sources in the Trapezium were not even detected at 5 mJy (5 σ level)). This result coupled with the HST optical observations of the proplyds suggests that circumstellar disks in the Trapezium OB association are being evaporated or destroyed. If we assume that the most massive disks in the Trapezium started out with masses as high as the most massive disks in NGC 2071 or Taurus (0.1 $M_\odot$), then we can estimate the mass loss rate and survival time for disks in the Trapezium environment.

$$mass\, loss\, rate\ = mass\, loss/cluster\ age\ =\ 0.1M_\odot\ /10^6 yr \sim 10^{-7} M_\odot yr^{-1}$$

This mass loss rate implies disk lifetimes in the Trapezium of only 10^6 years, significantly shorter than lifetimes for disks in isolated environments such as Taurus (Strom, Edwards & Skrutskie 1993) and too short to allow for the formation of planets. This further implies that environment and stellar content play important roles in determining the properties and survival of protoplanetary disks.

These results have important ramifications for the likelihood of planet formation in the Galaxy. If a significant number of stars are born in clusters containing O stars, forming planetary systems may be a difficult proposition. What factors impact the formation and survival of proto-planetary disks in clusters, the presence of O stars or high stellar density? Are disks more massive and do they have longer lifetimes in clusters without O star members? It is clearly important to investigate disk properties in clusters with differing age and stellar content in order to access the ability to form planets in clustered environments.

Acknowledgements

I thank the organizers of this NATO ASI, Charles Lada and Nick Kylafis for inviting me to participate in this very lively and enjoyable conference and thank the participants of the conference for many stimulating discussions. I am grateful to Joao Alves, Karl Haisch and Gus Muench for interesting discussions and for providing data in advance of publication. I would also like to thank Richard Elston for help preparing the figures.

References

Abt, H. 1983 *Ann. Rev. Astron. & Astrophys.*, 21, 343.
Adams, F. C. and Shu, F. H. 1986 *Astrophys. J.*, 308, 836.
Adams, F. C., Lada, C. J., and Shu, F. H. 1987 *Astrophys. J.*, 312, 788.
Allen, L. E. 1996, Ph.D. thesis, Univ. of Massachusetts at Amherst.
Alves, J. Lada, C. J., Lada, E. A., Kenyon, S. J., & Phelps, R. 1998 *Astrophys. J.*, 506, 292.
Alves, J. Lada, C. J. and Lada, E. A. 1999 in prep.
Beckwith, S.V.W., Sargent, A.I., Chini, R.S., & Guesten, R. 1990 *Astron. J.*99, 924.
Beckwith, S.V.W., and Sargent , A.I. 1991 *Astron. J.*, 381, 250.
Beckwith, S.V.W., and Sargent, A. I. 1993 in *Protostars and Planets III*, ed. E.H. Levy and J.I. Lunine, Univ. of Arizona Press. p. 521.
Blitz, L., & Stark, A. A. 1986 *Astrophys. J. Letters*, 300, L89.
Blitz, L. 1993 in *Protostars and Planets III*, ed. E.H. Levy and J.I. Lunine, University of Arizona Press, p.125 .
Bontemps, S. Andre, P. & Ward-Thompson, D. 1995, *Astron. & Astrophys.*, 297, 98.
Bovier, J., Rigaut, F., & Nadeau, D. 1997 *Astron. & Astrophys.*323, 139.
Carpenter, J. M., Snell, R. L., & Schloerb, F. P. 1995 *Astrophys. J.*, 450, 201.
Carpenter, J. M., Meyer, M., Dougados, C., Strom, S.E., Hillenbrand, L.A. 1997 *Astrophys. J.*, 114, 127.
Churchwell, E., Felli, M., Wood, D.O.S., & Massi, M. 1987 *Astrophys. J.*, 321, 516.
Clarke, C., and Pringle, J. 1991 *Monthly Notices Roy. Astron. Soc.*, 249, 588.
Comeron, F., Rieke, G.H., & Rieke, M.J 1996 *Astrophys. J.*, 473, 294.
Duchene, G., Bouvier, J., Simon, T. 1999 *Astron. & Astrophys.*, 343, 831.
Duquennoy, A. & Mayor, M. 1991 *Astron. & Astrophys.*248, 48.
Elmegreen, B., 1983 *Monthly Notices Roy. Astron. Soc.*, 203, 1011.
Elmegreen, B., & Clemens, C. 1985 *Astrophys. J.*, 294, 523.

Felli, M., Taylor, G.B., Catarzi, M., Churchwell, E., & Kurtz, S. 1993 *Astron. & Astrophys. Suppl.*101, 127.
Fletcher, A. B., & Stahler, S. W. 1994a *Astrophys. J.*, 435, 313.
Fletcher, A. B., & Stahler, S. W. 1994b *Astrophys. J.*, 435, 329.
Garay, G., Moran, J.M., & Reid, M.J. 1987 *Astrophys. J.*314, 535.
Ghez, A., Neugebauer, G., Matthews, K. 1993 *Astron. J.*106, 2005.
Gomez, M., Hartmann, L., Kenyon, S. L. & Hewitt, R. 1993 *Astron. J.*, 105, 1927.
Greene, T.P. & Young, E. T. 1992 *Astrophys. J.*395, 516.
Haisch, K., Lada, E. A. & Pina, R., 1999 to be submitted.
Haisch, K., Lada, E. A. & Lada, C. J., 1999 to be submitted.
Haisch, K., & Lada, E. A. 1999 in prep.
Hillenbrand, L,. Strom, S., Calvet, N., Merrill., K.M., Gately., I. Russell, B., Meyer, M. Skrutski, M. 1998 *Astron. J.*, 116, 1816.
Hills, 1980 *Astrophys. J.*, 235, 986.
Horner, D.J., Lada, E.A. & Lada, C. J., 1997 *Astron. J.*, 113, 1788.
Kenyon, S. J. & Hartmann, L. W. 1987 *Astrophys. J.*, 323, 714.
Kenyon, S. J. & Hartmann, L. W. 1995 *Astrophys. J. Suppl. Ser.*, 101, 117.
Kenyon, S. J., Hartmann, L.W., Strom, K.M., & Strom, S.E. 1990 *Astron. J.*, 99, 869.
Kramer, C., Stutzki, J., Rohrig, R., Corneliussen, U. 1998 *Astron. & Astrophys.*, 329 249.
Kroupa, P. 1995 *Monthly Notices Roy. Astron. Soc.*, 277, 1522.
Lada, C. J. and Wilking, B. A. 1984 *Astrophys. J.*, 287, 610.
Lada, C. J., Margulis, M. & Dearborn, D. 1984 *Astrophys. J.*, 285, 610.
Lada, C. J. 1987, IAU Symposium No. 115: Star Forming Regions, ed. M. Peimbert and J. Jugaku, (Reidel Press), pg. 1.
Lada, C. J. 1991 in *The Physics of Star Formation and Early Stellar Evolution* ed. C.J. Lada & N. D. Kylafis p.329.
Lada, C.J. & Lada, E. A. 1991 in *The Formation and Evolution of Star Clusters*, ed. K. Janes (ASP, San Francisco) p. 3.
Lada, C.J. & Adams, F.C. 1992 *Astrophys. J.*, 387, 572.
Lada, C. J., Lada, E. A., Clemens, D. P. & Bally, J. 1995 *Astrophys. J.*429, 694.
Lada, C. J., Alves, J. and Lada, E. A. 1996 *Astron. J.*, 111, 1964.
Lada, E. A., DePoy, D., Evans, N. J. and Gatley I. 1991 *Astrophys. J.*, 371, 171.
Lada, E. A., Bally, J. & Stark, A. 1991 *Astrophys. J.*, 368, 42.
Lada, E. A. 1992 *Astrophys. J. Letters*, 393, L25.
Lada, E. A., Strom, K. M. & Myers, P.C. 1993 in *Protostars and Planets III*, ed. E.H. Levy and J.I. Lunine, University of Arizona Press, p. 245.
Lada, E. A. & Lada, C. J. 1995 *Astron. J.*, 109, 1682.
Lada, E. A., Evans, N.J., & Falgarone, E. 1997, *Astrophys. J.*, 488, 286.
Lada, E. A. & Beckwith, 1999 *Astrophys. J.*in preparation.
Lada, E. A., Dutrey, A., Guilloteau, S., & Mundy, L. 1999 to be submitted.
Lada, E. A., & Dahari, D. 1999 in prep.
Larson, R. 1990, in *Physical Processes in Fragmentation and Star Formation*, ed. R. Capuzzo- Dolcetta, C. Chiosio, and A. Fazio, Kluwer, pp 389-399.
Leinert, C., Zinnecker, H., Weitzel, N., Cristou, J., Ridgeway, S.T., Jameson, R., Haas, M., & Lenzen, R. 1993 *Astron. & Astrophys.*, 278, 129.
Li, W., Evans, N.J., & Lada, E. A. 1997 *Astrophys. J.*, 488, 277.
Li, W., Evans, N.J., & Lada, E. A. 1998 *Astrophys. J.*to be submitted.
Mathieu, R., D. 1983 *Astrophys. J. Letters*, 267, 97.
Meyer, M. & Lada, E. A. 1999 in Orion Resisted ed. M McCaughrean (ASP, San Francisco) in press.
Mathis, J. 1990 *Ann. Rev. Astron. & Astrophys.*28, 37.
McCaughrean M.J., & Stauffer, J.R. 1994 *Astron. J.*, 108, 1382.
Megeath, S.T. 1996 *Astron. & Astrophys.*, 311, 135.
Muench, A., Lada, E.A. & Lada, C.J. 1999 *Astrophys. J.*submitted.
Mundy, L. G., Looney, L.W., & Lada. E.A., *Astrophys. J. Letters*, 452, 137.

Myers, P. C., Fuller, G. A., Mathieu, R. D., Beichman, C. A., Benson, P. J., Schild, R. E., & Emerson, J. P. 1987 *Astrophys. J.*, 319, 340.
O'Dell, C.R., Wen, Z. & Hu, X. 1993 *Astrophys. J.*410, 696.
O'Dell, C.R. & Wen, Z. 1994 /apj 436, 194.
Osterloh, M. & Beckwith, S.V.W. 1995 *Astrophys. J.*429, 288.
Patel, K., & Pudritz, R.E. 1994 *Astrophys. J.*424, 688.
Petr, M., Codude DU Foresto, V., Beckwith, S.V.W., Richichi, A., & McCaughrean, M. 1998 *Astrophys. J.*500, 825.
Phelps, R. L. and Lada, E. A. 1997 *Astrophys. J. Letters*, 477, 176.
Prosser, C., Stauffer, J.R., Hartmann, L., Soderblom, D., Jones, B.F., Werner, M.W. & McCaughrean, M.J. 1994 *Astrophys. J.*, 421, 517.
Reipurth, B. & Zinnecker, H. 1993 *Astron. & Astrophys.*, 278, 81.
Rieke, G. & Lebofsky, M. 1985 *Astrophys. J.*, 288, 618.
Roberts, 1957 *P.A.S.P.*, 69, 406.
Rydgren, A. E., and Zak, D. 1987 *P.A.S.P.*, 99, 141.
Rucinski, S. M., 1985 *Astron. J.*, 90, 2321.
Saiyadopour, A., Deiss, B. M., Kegel, W. 1997 *Astron. & Astrophys.*, 322, 756.
Shu, F., Najita, J., Galli, D., Ostriker, E., & Lizano, S. 1993 in *Protostars and Planets III*, ed. E.H. Levy and J.I. Lunine, Univ. of Arizona Press, p.3.
Simon, M., Ghez, A.M., Leinert, CH., Cassar, L., Chen.W.P., Howell, R.R., Jameson, R.F., Matthews, K., Neugebauer, G., Richichi, A. 1995 *Astrophys. J.*443, 625.
Skrutskie, M. F., Dutkevitch, D., Strom, S. E., Edwards, S., and Strom, K. M. 1990 *Astron. J.*, 99, 1187.
Strom, K. M., Strom, S. E., Kenyon, S. J., and Hartmann, L. 1988 *Astron. J.*, 95, 534.
Strom, K. M., Strom, S. E. and Merrill, K. M. 1993 *Astrophys. J.*, 412, 233.
Strom, S. E., Edwards, S. & Skrutskie, M. F. 1993 in *Protostars and Planets III*, ed. E.H. Levy and J.I. Lunine, Univ. of Arizona Press, p. 837.
Strom, S.E., Kepner, J., & Strom, K. M. 1995 *Astrophys. J.*, 438, 813.
Walter, F. M. 1987 *P.A.S.P.*, 99, 31.
Welch, J. & Sargent, A. I. 1993 *Ann. Rev. Astron. & Astrophys.*, 31, 297.
Verschueren, W. & David, M. 1989 *Astron. & Astrophys.*, 219, 105.
Verschueren, W. 1990 *Astron. & Astrophys.*, 234, 156.
Zinnecker, H., McCaughrean, M.J. & Wilking, B. A. 1993 in *Protostars and Planets III*, ed. E.H. Levy and J.I. Lunine, University of Arizona Press, p.429.